

Supporting Information

Theoretical Modeling of Tunneling Barriers in Carbon-based Molecular Electronic Junctions

Mykola Kondratenko^{1,2}, Stanislav R. Stoyanov^{1,3,4}, Sergey Gusarov¹, Andriy Kovalenko^{1,4}, Richard L. McCreery^{1,2*}

**Corresponding author, mcreery@ualberta.ca*

¹National Institute for Nanotechnology, National Research Council Canada, Edmonton, Alberta, Canada,

²Department of Chemistry, University of Alberta, Edmonton, Alberta, Canada

³Department of Chemical and Materials Engineering, University of Alberta, Edmonton, Alberta, Canada

⁴Department of Mechanical Engineering, University of Alberta, Edmonton, Alberta, Canada

1. Schematics of model calculations
2. Electron density distributions and orbital energies for 54-ring graphene
3. Electron density distributions for G54-Azobenzene orbitals HOMO to H-10
4. Dependence of H-X orbital energy on dihedral angle for eight molecules
5. Electron density distributions for azobenzene, ethynyl benzene, and bis(thienyl) benzene bonded to G54 with optimized and 33° dihedral angles.

1. Schematics of model calculations

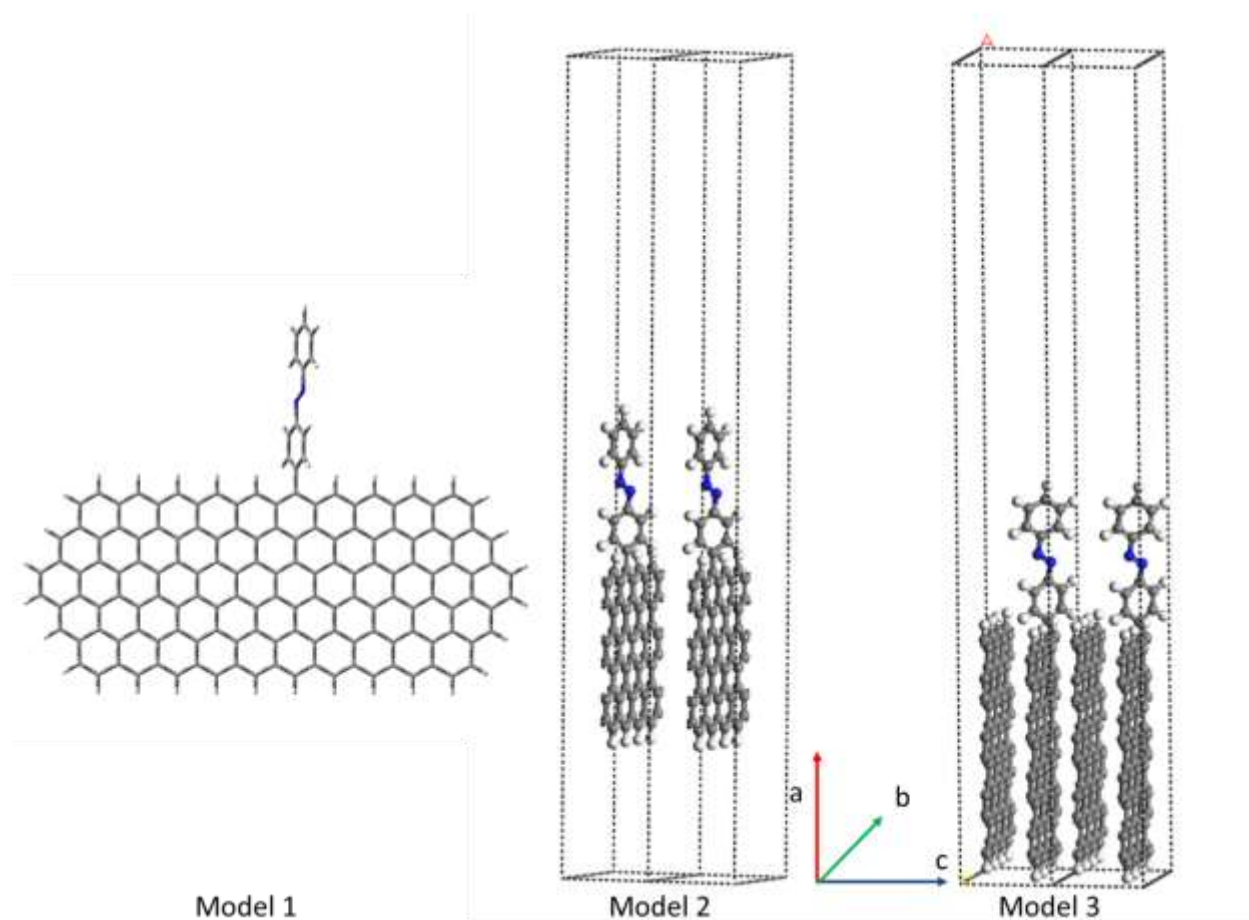


Figure S1. Schematic representation of three models (azobenzene example). For Models 2 and 3 the unit cell parameters used with periodic boundary conditions are: **a** (6.000 nm), **b** (0.984 nm) and **c** (0.680 nm).

2. Electron density distributions and orbital energies for 54-ring graphene

The first issue for constructing an accurate model is the size of the graphene sheet required to represent a conducting graphitic carbon material. The energies of the HOMO and LUMO of progressively larger H-terminated graphene sheets determined with DFT (i.e. Model 1) are shown in Figure S2, starting with benzene. The HOMO-LUMO gap decreases with the number of rings, until a slow increase is observed past 54 rings. Spatial distributions of the HOMO, H-1, LUMO, and L+1 orbitals of G54 are presented in Figure S3.

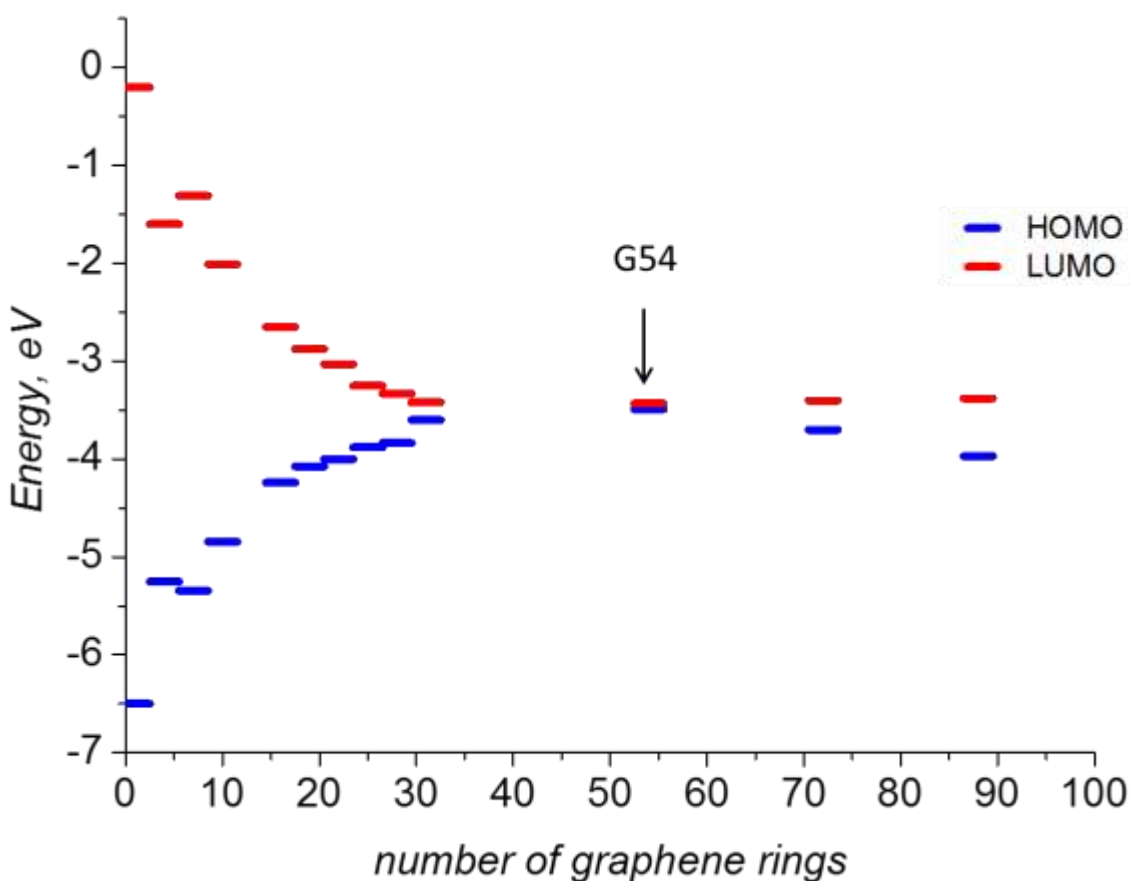


Figure S2. HOMO and LUMO energies for H-terminated graphene sheets of increasing size, relative to vacuum.

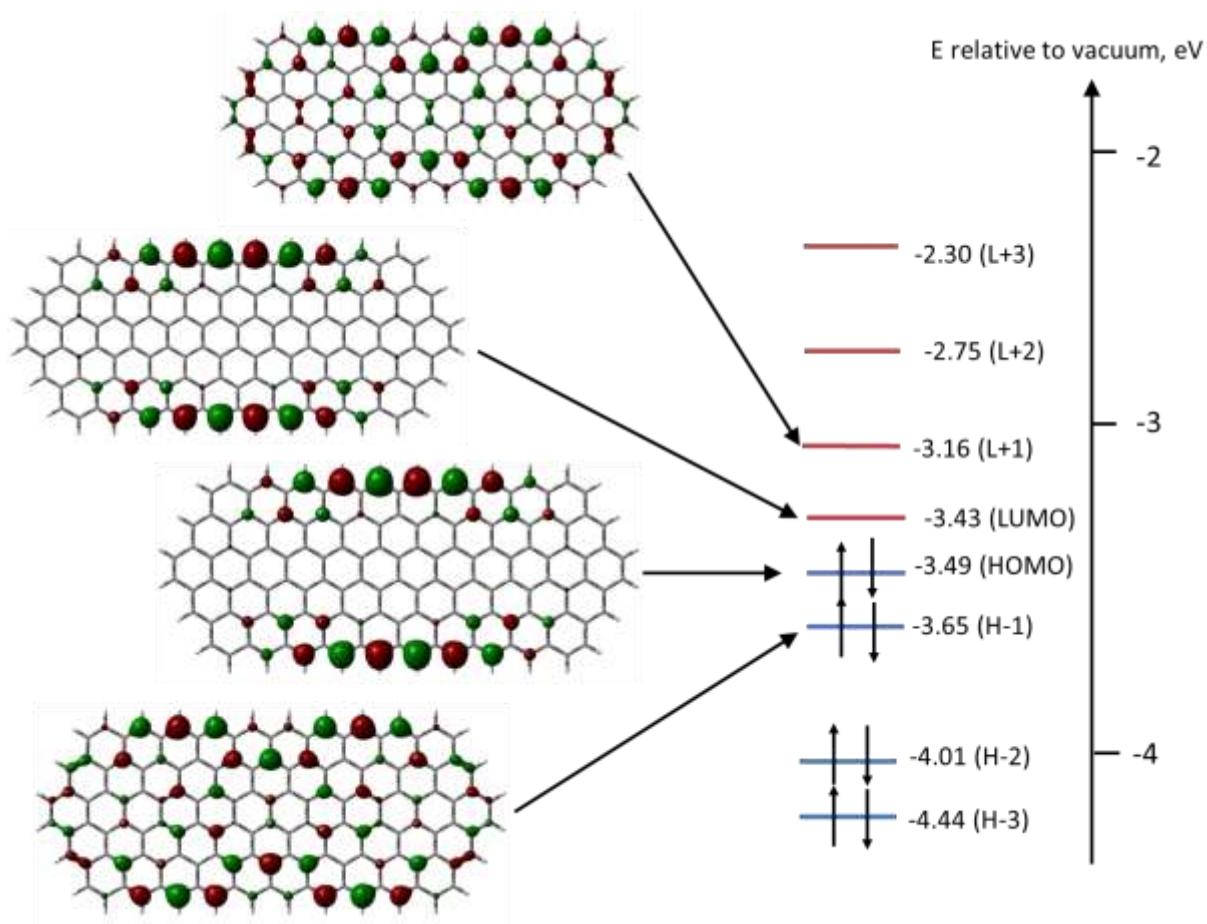


Figure S3. Electron density distributions and energies for selected orbitals in the G54 graphene sheet, using Model 1.

One of the most extensively studied theoretical analogs of sp^2 hybridized carbon is the graphene nanoribbon (GNR), consisting of elongated strips of single layer graphene with finite width and H atom termination. The GNRs can be either metallic or semiconducting, depending on the crystallographic ribbon axis. Theoretical calculations mainly based on tight-binding approximations predict that zigzag GNRs are always metallic while armchairs can be either metallic or semiconducting, depending on their width. Band-gap oscillations have also been predicted for semiconducting narrow armchair ribbons as a function of their width.¹ Computational studies show that GNRs with widths larger than 8 nm have a band gap of 0.3 eV while for structures wider than 80 nm the predicted band gap is 0.05 eV.² DFT calculations also show that armchair nanoribbons are semiconducting with an energy gap scaling with the inverse of the GNR width.² Experimental results show that the energy gaps do increase with decreasing GNR width.³

3. Electron density distributions for G54-Azobenzene orbitals HOMO to H-10

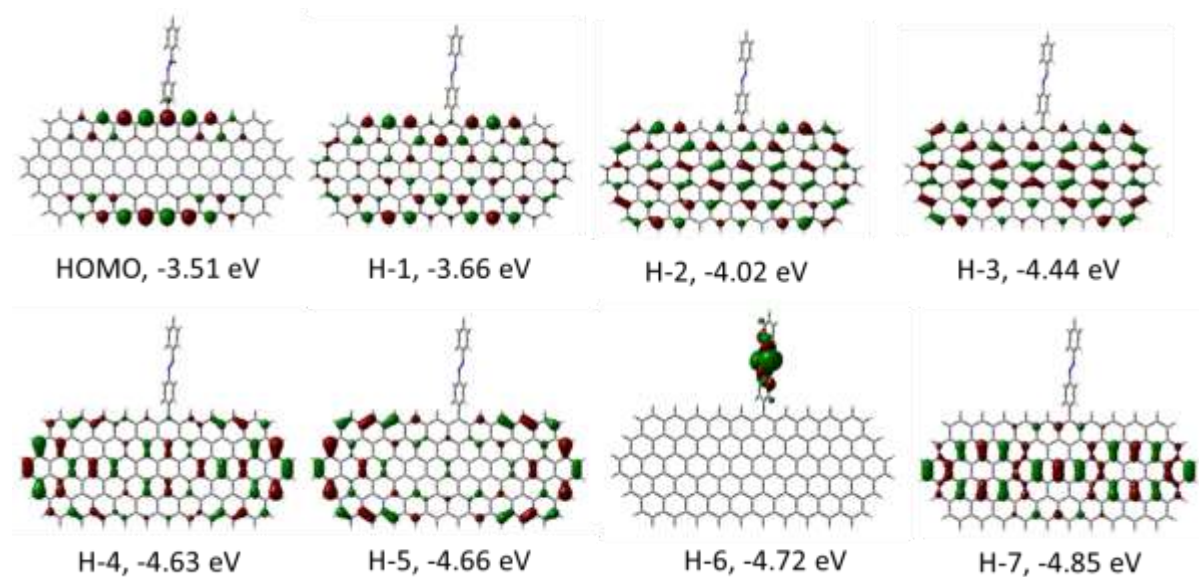


Figure S4. Electron density distributions and energies for HOMO and H-1 to H-7 orbitals for the G54-Azobenzene model system having the optimized dihedral angle of 65° using Model 1.

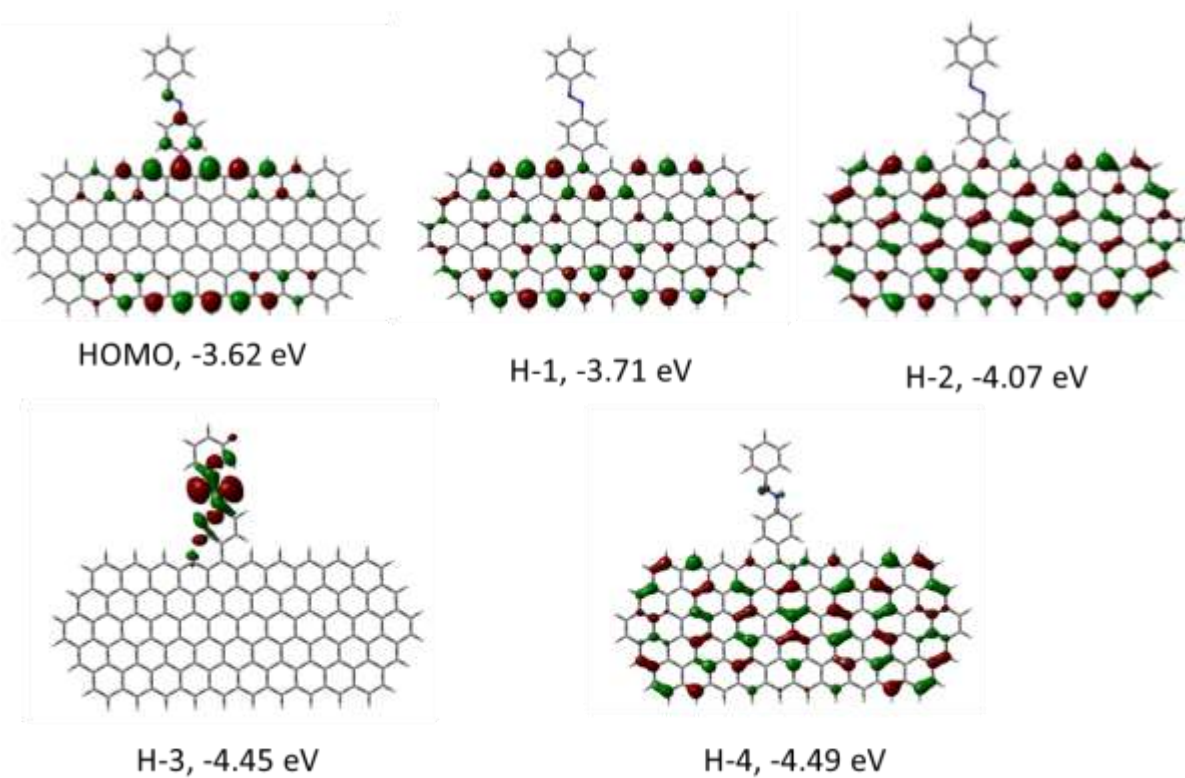


Figure S5. Same as Figure S4, but for the five highest energy orbitals of G54-AB optimized to its low energy configuration followed by forcing the dihedral angle to 0°

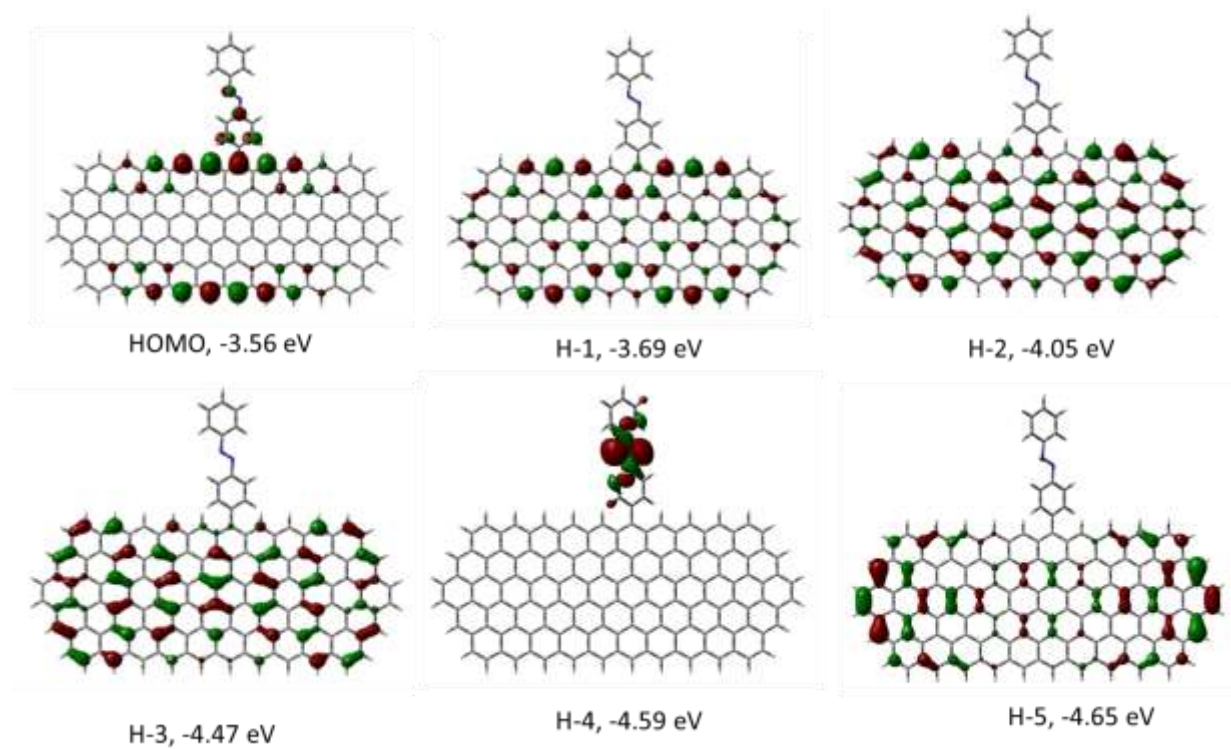


Figure S6. Same as Figure S4, for a forced dihedral angle of 33° , which is the optimized angle resulting from Model 3.

4. Dependence of H-X orbital energy on dihedral angle for eight molecules

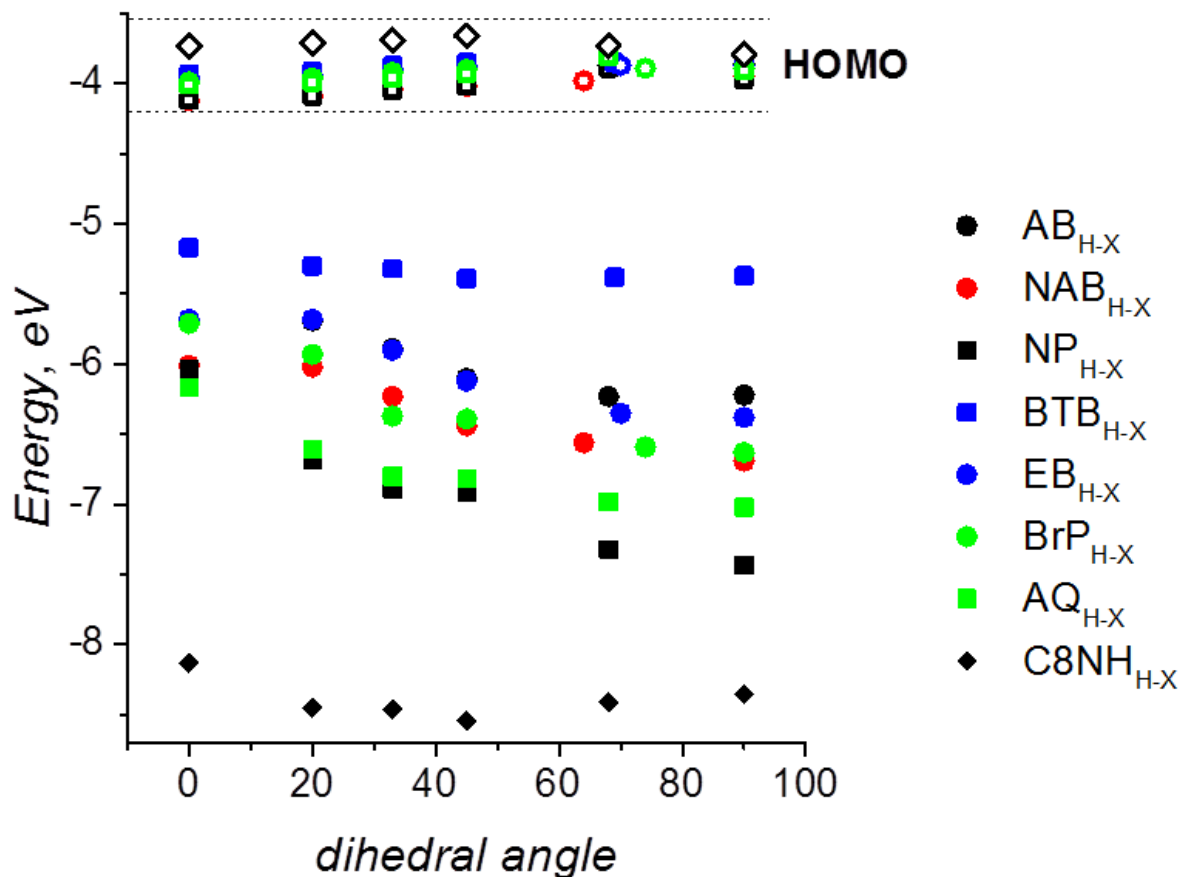


Figure S7. Orbital energies determined with Model 1 for the HOMOs and H-X orbitals of the indicated G54-molecule systems as a function of the dihedral angle between the G54 sheet and the plane of the aromatic molecule. AB= azobenzene, NAB= nitroazobenzene, BrP=bromophenyl, EB=ethynyl benzene, NP= nitrophenyl, AQ= anthraquinone, BTB= bisthienylbenzene, C8NH= octylamine. For octylamine, the dihedral angle is between the G54 plane and the plane of the C-C backbone of the alkyl group.

5. Electron density distributions for azobenzene, ethynyl benzene, and bis(thienyl) benzene bonded to G54 with optimized and 33° dihedral angles using Models 1, 2, and 3.

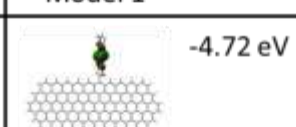
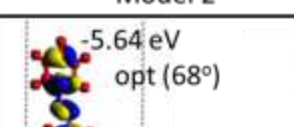
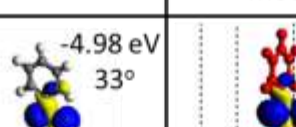
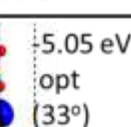
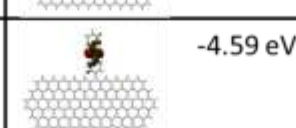
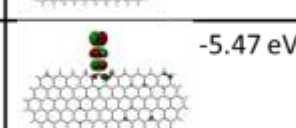
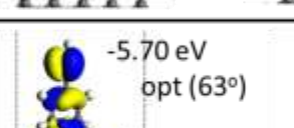
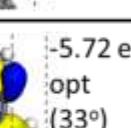
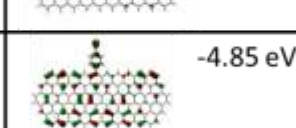
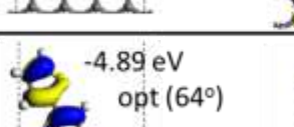
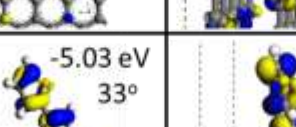
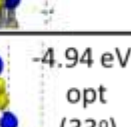
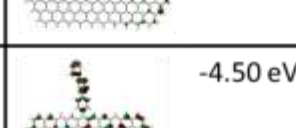
| | Model 1 | Model 2 | Model 3 | |
|---------------|--|--|---|--|
| AB opt (65°) |  -4.72 eV |  -5.64 eV opt (68°) |  -4.98 eV 33° |  5.05 eV opt (33°) |
| AB 33° |  -4.59 eV | | | |
| EB opt (69°) |  -5.47 eV |  -5.70 eV opt (63°) |  -5.73 eV 33° |  -5.72 eV opt (33°) |
| EB 33° |  -4.85 eV | | | |
| BTB opt (68°) |  -4.48 eV |  -4.89 eV opt (64°) |  -5.03 eV 33° |  -4.94 eV opt (33°) |
| BTB 33° |  -4.50 eV | | | |

Figure S8. Examples illustrating the effects of dihedral angle on orbital energies and electron density distributions. “Opt” indicates the low energy configuration, and 33° is the low energy angle resulting from Model 3, which most closely approximates the real PPF-molecule system.

- (1) Ezawa, M. Peculiar Width Dependence of the Electronic Properties of Carbon Nanoribbons. *Phys. Rev. B* **2006**, *73*, 045432.
- (2) Barone, V.; Hod, O.; Scuseria, G. E. Electronic Structure and Stability of Semiconducting Graphene Nanoribbons. *Nano Lett.* **2006**, *6*, 2748-2754.
- (3) Han, M. Y.; Ozyilmaz, B.; Zhang, Y. B.; Kim, P. Energy Band-Gap Engineering of Graphene Nanoribbons. *Phys. Rev. Lett.* **2007**, *98*, 206805.